



Published in final edited form as:

*PET Clin.* 2016 October ; 11(4): 387–402. doi:10.1016/j.cpet.2016.05.008.

## Clinical PET-MR Imaging in Breast Cancer and Lung Cancer

**Samuel L. Rice, MD and Kent P. Friedman, MD\***

Division of Nuclear Medicine, Department of Radiology, New York University Langone Medical Center, 660 First Avenue, New York, NY 10016, USA

### Keywords

PET-MR imaging; Hybrid imaging; Breast cancer; Lung cancer; Oncology; Thoracic imaging

### INTRODUCTION

Advances in radiographic computed tomography (CT), MR imaging, PET, and combined PET-CT have dramatically improved the management of patients with cancer over the past 2 decades. For years, researchers and clinicians have wondered if combining PET with MR imaging would offer similar or even greater advantages compared with PET-CT.

Recent advancements in MR imaging scanners and the advent of MR imaging-compatible solid-state PET detectors that replace traditional photomultiplier tubes have made it possible to finally combine MR imaging and PET into a single device that acquires whole-body PET-MR images. Potential advantages of hybrid PET-MR imaging compared with PET-CT include superior identification of lesions in the brain, breast, liver, kidney, and bones, as well as enhanced evaluation of the margins of lesions. Improved anatomic registration with PET secondary to simultaneous image acquisition is now a reality with the advent of simultaneous PET-MR imaging scanners. Furthermore, the application of multiparametric quantitative imaging in MR imaging and functional PET has the potential to better guide patient management and to decrease the number of imaging studies required for clinical decision-making, resulting in less radiation exposure and improved patient satisfaction (Box 1).

Neoplasms of the thorax, including those of the breast and lung, are some of the most commonly diagnosed cancers in the western world, which cause exceptionally high morbidity and mortality and are areas of active study in the emerging field of clinical PET-MR imaging. According to cancer statistics in 2015, approximately 234,190 people were diagnosed with breast cancer and 221,200 were diagnosed with lung neoplasms in the United States; this includes an estimated 40,730 and 158,040 related deaths secondary to these 2 diseases, respectively.<sup>1</sup> Overall survival is greatly influenced by the stage of the neoplasm at the time of diagnosis and by the histologic subtype of cancer.

---

\*Corresponding author: kent.friedman@nyumc.org.

The authors have nothing to disclose.

PET systems have greatly improved in the last few decades with faster imaging time and improved scanner resolution; the combination of CT with hybrid PET-CT scanners has merged anatomic and molecular imaging, allowing for more accurate diagnosis and staging of many neoplasms. <sup>18</sup>F- 2-fluoro-2-deoxy-D-glucose (FDG) is a radioactive analogue of glucose and the most commonly used PET radiotracer in clinical practice. The clinical implementation of multiple novel clinical PET radiotracers, along with ongoing research of various others, has advanced and improved the potential molecular imaging capabilities of PET, accurately permitting in vivo imaging of various important clinical markers, including cell surface receptor expression, DNA production or repair, and hypoxia.<sup>2,3</sup> MR imaging has also evolved with new and faster sequences that allow for whole-body imaging, as well as functional imaging sequences, including magnetic resonance spectroscopy (MRS), perfusion imaging, and diffusion-weighted imaging (DWI), which have expanded the use of MR imaging in characterizing disease. With all of the added benefits of combined PET-MR imaging, the imaging algorithm currently used for thoracic cancers can be further optimized, potentially allowing for superior clinical information to be obtained from a single scan (Box 2).

## PET-COMPUTED TOMOGRAPHY IN BREAST CANCER

Breast cancer remains exceedingly prevalent in the Western world and is a leading cause of mortality in women. Once diagnosed, survival is inversely related to the extent of disease at diagnosis, currently characterized with the tumor-node-metastasis (TNM) staging system. Metastases to axillary lymph nodes have a profound influence on patient prognosis, with 10-year survival ranging from 90% without the presence of lymphatic spread down to 30% when greater than 10 lymph nodes are involved.<sup>4</sup> Currently, the primary role of FDG PET-CT in patients with breast cancer is for assessment of suspected tumor recurrence or staging of locally advanced disease (ie, with large primary tumors >50 mm in size, chest wall tumor involvement, or axillary, internal mammary, or infraclavicular or supraclavicular lymph node metastases). Evidence exists that patients with inflammatory breast cancer also benefit from early FDG PET-CT imaging.<sup>4-6</sup>

Current guidelines for initial staging of breast cancer include physical examination, biopsy with histologic evaluation, and an array of imaging modalities, including mammography, ultrasonography, MR imaging, and potentially FDG PET-CT. The sensitivity of FDG PET-CT for small tumors less than 10 mm (T1 stage) has been shown to range from 50% to 72%, with the sensitivity of FDG PET-CT increasing to greater than 90% for tumors between 20 to 50 mm.<sup>7-9</sup> FDG PET-CT has been shown to underestimate the extent of disease within the breast when compared with MR imaging, with the accuracy of correctly diagnosing the degree of primary disease in the breast found to be 54% and 77%, respectively, for these 2 imaging modalities.<sup>8,10,11</sup> The poor performance of whole-body FDG PET-CT in evaluating primary tumors in the breast can be attributed to volume averaging due to the small size of the lesion, the generally lower hexokinase activity of breast cancer when compared with other cancer types, variations in tumor FDG uptake secondary to histologic subtype, and the background FDG uptake of normal breast tissue.<sup>12-14</sup> FDG PET-CT for the assessment of lymph node disease has a sensitivity, specificity, positive predictive value, and negative predictive value of 61%, 80%, 62%, and 79%, respectively.<sup>15</sup> This underestimation of the

number of lymph nodes involved precludes it from replacing sentinel lymph node biopsy for primary evaluation of local spread and micrometastatic disease.

There has been extensive research in the use of changes in FDG uptake measured by standardized uptake value (SUV) within the tumor to assess for treatment response. Multiple studies have observed a statistically significant decrease in tumor FDG uptake in patients who have responded to therapy compared with those who have had no response. Evidence has also been presented that changes in SUV correlate with pathologic response to therapy.<sup>16-19</sup> Currently, clinicians use these changes to guide management decisions although determination of how to best leverage PET data in the setting of myriad cytostatic treatment options remains an area of active research (Box 3).

FDG PET-CT has also been validated for the accurate detection of recurrent breast cancer irrespective of histologic subtype with a sensitivity of 92% to 96% and a specificity of 75% to 90%.<sup>19-22</sup>

## MR IMAGING IN BREAST CANCER

MR imaging is a highly utilized imaging modality for the evaluation of breast lesions in conjunction with mammography and ultrasonography. MR imaging is currently used and approved for a number of purposes, including screening in women considered to be at high risk for disease (ie, lifetime risk >20%), assessment of patients with prior breast augmentation surgery, evaluation of the extent of disease in newly diagnosed patients (multifocal vs multicentric disease, chest wall invasion), and evaluation of response in patients who received neoadjuvant chemotherapy.<sup>23,24</sup>

Breast MR imaging typically uses a 1.5 or 3.0 T scanner; the patient is placed in the prone position with a dedicated breast coil used to acquire images with chemical fat suppression. Precontrast and postcontrast T1-weighted images are obtained using a gradient echo technique. Detection of neoplasms within the breast is primarily achieved by evaluating the dynamic contrast enhancement of a lesion in which the variable uptake kinetics of contrast material help to distinguish malignant from benign lesions.<sup>25</sup> Various other techniques have been used to improve the specificity of diagnosis, including the use of other imaging characteristics of a lesion. On MR imaging, the findings of rapid or medium initial contrast uptake (type II and III kinetic curves) or contrast washout on delayed phase images within lesions have a 77% positive predictive value for malignancy.<sup>26-28</sup> MR imaging is able to detect tumors at 10 mm, which is smaller than other commonly used imaging techniques.<sup>29-31</sup> MR imaging has also been shown to be highly sensitive but not specific, with a negative predictive value of 95% but a specificity of only 25%. A limitation of MR imaging of the breast includes normal cyclic changes in background breast tissue parenchymal enhancement by changing hormonal status of the patient, which limits its usefulness in younger patients but increases its specificity in postmenopausal women.<sup>26-28</sup>

Breast MR imaging can also be used to evaluate lymph node involvement by identifying an increase in size, increased contrast enhancement, and lack of a normal fatty hilum. MR imaging has a sensitivity and specificity of 90% and 82%, respectively, for the detection of

metastatic disease in lymph nodes when using size greater than 5 mm and abnormally increased enhancement.<sup>32</sup> A limitation to evaluating lymph nodes in the axilla is that standard breast coils have inadequate coverage of the axilla. Whole-body MR imaging is not used regularly for the evaluation of systemic metastatic disease or distant tumor recurrence.

## PET-MR IMAGING IN BREAST CANCER

The theoretical advantages of PET-MR imaging compared with PET-CT or MR imaging alone are just starting to be explored in preliminary clinical research. Much early work has focused on studies of technical feasibility and reproducibility of SUV quantification between PET-MR imaging and PET-CT. Early data are emerging that suggest a potential additive clinical value of PET-MR imaging and which may serve as the basis for larger studies. It is likely that to prove any further increase in diagnostic accuracy of PET-MR imaging compared with PET-CT, large multi-institutional trials will be required to assess for statistically significant incremental increases in sensitivity or specificity.

Many questions exist regarding quantitative differences with respect to SUV obtained from PET-CT and PET-MR imaging. Whereas CT-based attenuation correction directly measures attenuation throughout the body, current MR imaging-based attenuation correction algorithms use methods to segment tissues into basic categories, including fat, soft tissue, air, and lung parenchyma. Some newer techniques are emerging that seek to map the locations of bones. All of these techniques are based on fixed estimates of tissue density that may or may not reflect the clinical reality for individual patients. Lung density is challenging to measure or estimate on MR imaging, and is variable in individual patients. Breast density may change with surgery or placement of prosthetics, and all of these factors may potentially affect SUV quantification in the evaluation of patients with breast cancer.

## STANDARDIZED UPTAKE VALUE: PET-MR IMAGING VERSUS PET-COMPUTED TOMOGRAPHY IN BREAST CANCER

Preliminary work has demonstrated good correlation between SUV measured on PET-MR imaging compared with PET-CT. Most studies compare values by scanning patients first on PET-CT and then on PET-MR imaging. This leads to a time delay between the 2 PET datasets and changes in physiologic concentrations of the radiotracer, which very likely affects the results independent of scanner performance. In 2014, Pace and colleagues<sup>33</sup> reviewed SUV measurements in patients with breast cancer scanned on PET-CT followed by PET-MR imaging an hour later using 2-point Dixon MR imaging sequences that generated a 4 tissue-class attenuation correction map (fat, soft tissue, lungs, air). They found that subjective assessment of lesion localization to anatomic structures was the same between PET-CT and PET-MR imaging. Primary tumors and lymph node uptake was visually scored as having slightly higher contrast on PET-MR imaging. With respect to SUV quantification, the investigators found a significantly higher maximum SUV (SUVmax) for lymph nodes and metastases and no significant change in SUVmax for primary tumors when comparing PET-MR imaging with PET-CT. They found a significantly lower SUV on PET-MR imaging for normal lung, liver, and muscle; no significant difference for spleen; and a higher SUV for left ventricular myocardium. The investigators suggest that these SUV differences likely

reflect a combination of time-dependent physiologic and technical scanner factors, and the study design does not allow determination of the impact of the scanner technology alone. They conclude that PET-MR imaging can be used for quantitative analysis in clinical settings but warn that SUV measurements between PET-CT and PET-MR imaging may not be comparable.<sup>33</sup>

In a similar 2015 study by Sawicki and colleagues,<sup>34</sup> 21 subjects with recurrent breast cancer underwent FDG PET-MR imaging immediately following PET-CT. The investigators found a mild but statistically significant increase in SUV on PET-MR imaging for all tumor deposits (SUV<sub>max</sub>  $5.6 \pm 2.8$  for PET-MR imaging vs  $4.9 \pm 1.8$  for PET-CT) with strong and significant correlation ( $r = 0.72$ ,  $P < .001$ ). Pujara and colleagues<sup>35</sup> studied 35 subjects who underwent FDG PET-CT followed by PET-MR imaging and found statistically significant correlations of SUV measurements for lesions within bone marrow, liver, and lymph nodes ( $r = 0.74$ – $0.95$ ). They found no statistically significant difference in SUV measurements overall for bone marrow metastases or for lymph node metastases. However, there was a significant difference in average SUV<sub>max</sub> for liver metastases ( $4.96 \pm 3.04$  for PET-MR imaging vs  $7.79 \pm 5.78$  for PET-CT;  $P < .05$ ). To what extent this is secondary to segmentation error, tissue attenuation value variability (compared with reality), or time-dependent physiologic differences between PET-CT and PET-MR imaging is uncertain. In contrast to prior studies, PET-MR imaging average SUV<sub>max</sub> measurements were slightly lower (eg,  $6.25 \pm 4.91$  for PET-MR imaging vs  $6.99 \pm 4.63$  for PET-CT), as were values (as expected) for normal structures ( $1.15 \pm 1.37$  vs  $1.60 \pm 1.35$ ).

## PET-MR IMAGING LESION DETECTION IN BREAST CANCER

A potential advantage of PET-MR imaging compared with PET-CT is in leveraging the MR imaging data to improve lesion detectability. It remains an open question whether or not additional lesion detection with PET-MR imaging will be statistically significant, economically beneficial (in light of the cost of PET-MR imaging), and most importantly advantageous enough to improve patient management decisions and patient outcomes.

In the aforementioned study by Pace and colleagues,<sup>33</sup> lesion detection rates for PET-CT versus PET-MR imaging were reported for 36 subjects undergoing FDG PET-MR imaging following PET-CT. All 74 FDG-avid lesions seen on PET-CT were also visible on PET-MR imaging, including 25 primary tumors, 35 metastatic nodes, and 14 distant metastases. In a study comparing the performance of FDG PET-MR imaging, FDG PET-CT, MR imaging, and CT in the setting of suspected recurrent breast cancer, PET-MR imaging detected 134 lesions, of which 97%, 96%, and 75% were seen on PET-CT, MR imaging, and CT, respectively. The performance of PET-MR imaging and PET-CT for detection of disease recurrence on a per-patient basis is equivalent. On a per-lesion basis, PET-CT was noted to miss 4 bone marrow metastases that were highlighted by the MR imaging portion of PET-MR imaging and found to have some focal FDG uptake that was not initially interpreted as tumor on PET-CT. The investigators note that a limitation of their study was a lack of lung metastases in their subject population, and that small lung lesions can be missed on PET and MR imaging.<sup>34</sup> In a more recent study by Pujara and colleagues<sup>35</sup> that focused on SUV quantification more than analysis of lesions detected, it was noted that during un-blinded

review, PET-CT initially detected 15 of 16 bone marrow metastases, 6 of 7 liver metastases, and 8 of 8 nonaxillary lymph node metastases that were detected on PET-MR imaging. Therefore, this study further suggests the potential for PET-MR imaging to detect bone marrow and potentially liver metastases that are missed on PET-CT. Finally, Melsaether and colleagues,<sup>36</sup> recently published a formal analysis of 242 distant metastatic lesions, 18 primary breast cancers, and 19 axillary nodes. They found that PET-MR imaging with DWI and contrast-enhanced sequences yielded better sensitivity for liver and possibly bone marrow metastases but potentially worse sensitivity for lung metastases.

Finally, it is worth noting that novel techniques for radiotracer injection may potentially be synergistic, with the added value possibly provided by MR imaging during clinical PET-MR imaging. In 2015, Minamimoto and colleagues<sup>37</sup> reported on a dual-radiotracer technique combining <sup>18</sup>F-labeled sodium fluoride (<sup>18</sup>F-NaF) and FDG injections during PET-CT compared with bone scintigraphy and whole-body MR imaging. The investigators found that combined <sup>18</sup>F-NaF-FDG PET-CT offered higher sensitivity for osseous metastasis detection compared with whole-body MR imaging alone but no significant difference compared with a combined read of whole-body MR imaging and bone scintigraphy. In a follow-up abstract published in 2015, the same group published preliminary findings of combined <sup>18</sup>F-NaF-FDG PET-MR imaging on a time-of-flight scanner compared with routine bone scintigraphy. Among subjects with osseous metastases, both bone scintigraphy and PET-MR imaging detected lesions. However, more numerous osseous findings were noted on PET-MR imaging in 3 subjects and lesions outside of the skeleton were found on PET-MR imaging in 2 subjects that were not visible on bone scan.<sup>38</sup> A logical follow-up study would be to compare dual-radiotracer PET-MR imaging to PET-CT and bone scintigraphy.

## TUMOR STAGING IN BREAST CANCER

There is scant literature directly addressing the possible synergy of PET and MR imaging for T staging of breast cancer. From a technical standpoint, a focused study of the breast is now possible with the advent of PET-MR imaging-compatible breast coils.<sup>39</sup> Although FDG PET is unlikely to improve sensitivity for detection of breast lesions, previously reported improvements in specificity might help to direct biopsies towards areas of more aggressive tumor histology.<sup>40</sup>

## ADDITIONAL PET-MR IMAGING APPLICATIONS IN BREAST CANCER: MULTIPARAMETRIC DATASETS

There are few existing data to assess the potential synergistic effects of combining PET and MR imaging quantitative data obtained during a single examination. In a 2014 study by Baba and colleagues,<sup>41</sup> subjects with newly diagnosed breast cancer underwent FDG PET and separate diagnostic breast MR imaging with DWI, and calculation of apparent diffusion coefficient (ADC). A weak inverse correlation between SUV and ADC was reported, and the investigators found that the ratio of SUV to ADC provided very slightly higher accuracy for differentiating between benign and malignant lesions. Unfortunately, this combined parameter did not perform better than SUV or ADC alone in the prediction of overall survival. Miyake and colleagues<sup>42</sup> reported that SUVmax and ADC both change during

treatment response before changes in tumor volume are apparent. Finally, Lim and colleagues<sup>43</sup> have demonstrated that a slower decline in SUV, a lesser decline in MR imaging slope on dynamic contrast-enhanced (DCE) MR imaging, and a lower increase in ADC was associated with worse prognosis after the first cycle of neoadjuvant chemotherapy.

Combining these data in a synergistic manner on PET-MR imaging to justify this new technology remains a significant challenge. Future research directions may leverage the ability of PET-MR imaging to acquire kinetic PET data and perform voxelwise correlations between multiparametric datasets with precise image registration and quantitative accuracy. Large-scale multi-institutional studies with advanced data analysis techniques may offer new insights into understanding the significance of the quantitative data that can be obtained from PET-MR imaging. Figs. 1–3 give examples of PET-MR imaging in patients with breast cancer.

## PET-COMPUTED TOMOGRAPHY IN LUNG CANCER

Lung cancer remains the most deadly neoplasm in the United States, affecting both men and women and causing approximately 162,000 deaths in 2015.<sup>1</sup> Lung neoplasms are divided into non-small cell lung cancer (NSCLC) and small cell lung cancer (SCLC). The treatment and prognosis is greatly influenced by tumor type and stage at diagnosis. Evaluation of lung neoplasms has typically been performed using CT to characterize them as malignant, as well as to assess therapeutic response based on lesion change in size on serial imaging. Other imaging characteristics, including shape, edge, cavitation, and location, have not been shown to be as reliable for these purposes.<sup>44,45</sup> Based on lesion size seen on CT alone, 6% to 28% of nodules measuring 5 to 10 mm turn out to be malignant based on subsequent evaluation with invasive procedures or follow-up imaging, with the time interval for follow-up evaluation leading to a delay in the initiation of therapy.<sup>46</sup> The advent of hybrid PET-CT with FDG has an expanding role in this disease given its ability to add functional metabolic information about the tumor to assist in earlier clinical assessment.<sup>47</sup>

FDG PET-CT has been suggested to improve T staging of lung cancer compared with CT alone, particularly for tumors surrounded by atelectasis or abutting the chest wall or mediastinum.<sup>48</sup> FDG PET-CT is both highly sensitive and specific for the diagnosis of pulmonary malignancy.<sup>49–51</sup> However, the sensitivity is lower for small and/or low-attenuation lung cancers, for which morphologic features detected on CT provide an increased role in patient management. The presence or absence of increased radiotracer uptake has the potential to prevent or redirect invasive procedures such as biopsy or resection for histologic sampling. Limitations to the accuracy of FDG PET-CT imaging in lung cancer are similar to other forms of cancer, including false-positive results due to inflammatory or infectious causes and false-negative results within small lesions due to the known lower sensitivity for tumors measuring less than 8 mm.<sup>49</sup> Histologic subtype also influences the uptake of radiotracer, with carcinoid and minimally invasive neoplasms possessing a smaller amount of uptake compared with SCLC, leading to lower detection rates on PET-CT.<sup>52–55</sup>

FDG PET-CT has been shown to be useful for diagnosing the spread of lung cancer into hilar, mediastinal, and supraclavicular lymph nodes, in addition to detecting invasion of tumor into the chest wall and mediastinum.<sup>56–59</sup> The sensitivity, specificity, positive predictive value, negative predictive value, and accuracy for detecting nodal spread is 54%, 92%, 74%, 82%, and 81%, respectively, for FDG PET-CT.<sup>60</sup> FDG PET-CT provides additional clinical benefit by guiding selection of the best invasive procedure for lymph node staging.

The incidence of metastasis at the time of diagnosis for lung cancer is high. The most common sites of disease spread are the adrenal glands, bone marrow, liver, and brain. FDG PET-CT has a sensitivity of 100% and a specificity of 80% to 100% for metastatic spread to the adrenal glands.<sup>61,62</sup> For bone marrow metastatic disease, FDG PET has been found to have a similarly high sensitivity for detection of lesions versus conventional bone scintigraphy but with a much higher specificity.<sup>63</sup>

In previously treated patients, the earlier tumor progression can be detected, the faster alternative therapies can be initiated. The potential to monitor treatment response to cytostatic or cytotoxic agents using metabolic markers has many advantages compared to evaluating anatomic changes in tumor size alone. One example of this is in the evaluation of postsurgical patients for which FDG PET-CT can be used to differentiate atelectasis or posttreatment scarring from active tumor recurrence. FDG PET-CT can detect recurrence with a sensitivity of 98% to 100% and a specificity of 62% to 92%.<sup>64,65</sup>

## MR IMAGING IN LUNG CANCER

Limitations exist for the use of MR imaging in evaluation of nodules within the lung parenchyma because of the susceptibility artifacts created by air within the lung, low signal-to-noise ratio of aerated lung, and motion artifacts from breathing during image acquisition.<sup>66–69</sup> Several solutions have been proposed to help alleviate these problems, including improved MR imaging hardware, application of novel phased-array receiver coils, the use of newer, faster imaging sequences, including fast spin echo and half-Fourier single-shot turbo spin echo (HASTE) T2-weighted sequences, and DWI.<sup>68–70</sup> The sensitivity of the T2-weighted HASTE MR imaging sequence to detect nodules less than 3 mm, 3 to 5 mm, 5 to 10 mm, and greater than 10 mm has been reported to be 73%, 86%, 96%, and 100%, respectively.<sup>71</sup> In a recent comparison with noncontrast CT and MR imaging using a respiratory-triggered short tau inversion recovery (STIR) MR imaging sequence, there was no difference in the detection of malignant nodules between the 2 sequences, even with the inferior spatial resolution and lower overall nodule detection of MR imaging.<sup>72</sup> DCE MR imaging is another method in development to help differentiate benign versus malignant lung lesions and to evaluate tumor neoangiogenesis.<sup>73,74</sup>

DWI and ADC map images, in which the movement of water molecules within a tissue is measured to determine its cellularity and tissue disorganization, have a sensitivity and specificity of 70% to 89% and 61% to 97%, respectively, in determining the presence of lung neoplasms.<sup>75</sup> The use of dynamic MR imaging techniques has been shown to



accurately distinguish malignant from benign lymph nodes with a sensitivity of 94% to 100% and a specificity of 70% to 96%.<sup>75-77</sup>

Due to its improved soft tissue contrast, MR imaging is useful to evaluate tumors in particular areas of the thorax, providing an especially robust modality for diagnostic evaluation. Such tumors include those adjacent to the superior sulcus, where involvement of the chest wall and brachial plexus by tumor can be best appraised by MR imaging, as well as those in the paramediastinal location, in which the relationship with the heart or large vessels is of importance.<sup>78</sup>

## PET-MR IMAGING IN LUNG CANCER

Lung cancer is challenging as a diagnostic application for PET-MR imaging due to the known limitations of MR imaging for detection of small and/or low attenuation lung nodules and also due to respiratory motion artifacts that occur in PET and MR imaging. Despite these challenges, potential advantages with respect to chest wall and mediastinal tumor evaluation, combined with the ability of MR imaging to detect brain, bone marrow, adrenal gland, and liver metastases not visible on PET-CT, yields ample room for study of this new modality. Opportunities for gated imaging without additional CT radiation to increase quantitative accuracy of PET and MR imaging data are also potential areas for future research.

## STANDARDIZED UPTAKE VALUE: PET-MR IMAGING VERSUS PET-COMPUTED TOMOGRAPHY IN LUNG CANCER

There are currently limited data regarding SUV quantification in lung cancer on PET-MR imaging compared with PET-CT. Given that current clinical PET-MR imaging scanners use a tissue-classification system for estimation of lung density compared with direct measurements obtained on PET-CT, some quantitative differences are expected. In a study focusing on lung nodule detection, Chandarana and colleagues<sup>79</sup> reported that for subjects undergoing PET-MR imaging after PET-CT, SUVmax measurements of lung nodules on PET-MR imaging versus PET-CT were strongly correlated ( $r = 0.96$ ,  $P < .001$ ) and overall average SUVmax was  $16.4 \pm 13.6\%$  higher on PET-MR imaging compared with PET-CT. To what extent this difference reflects the more delayed time point of imaging versus differences in attenuation correction factors is not entirely clear. In another study focusing on N staging in which PET-MR imaging was performed after PET-CT, Kohan and colleagues<sup>80</sup> reported that FDG-avid lymph node SUVmax increased from an average of 4.60 on PET-CT up to 5.85 on PET-MR imaging (27.27% higher), with a strong correlation ( $r = 0.93$ ) again observed. Although most SUV measurements were higher, the investigators point out that misclassification of soft tissue as air in some regions on the MR imaging attenuation map can lead to underestimation of true SUV.

## PET-MR IMAGING LESION DETECTION IN LUNG CANCER

Primary tumor detection rates for PET-MR imaging are of interest to clinicians managing patients with lung cancer. It is hypothesized that small lung nodules may be harder to

visualize on PET-MR imaging compared with PET-CT based on the known differences between CT and MR imaging. On the other hand, lung cancer has a tendency to spread to the brain, adrenal glands, and bone marrow, which are all areas where MR imaging may potentially perform better. It is, therefore, possible that MR imaging will detect metabolically inactive or minimally active metastases that are missed on PET-CT.

An initial comparison between PET-CT and PET-MR imaging for primary tumor detection noted similar detection rates for primary tumors between the 2 modalities, with identical T staging.<sup>81</sup> With respect to smaller nodules, the performance of PET-MR imaging was worse than PET-CT in a subsequent study by Chandarana and colleagues,<sup>79</sup> for which the sensitivity of PET-MR imaging was 96% for FDG-avid nodules, 70% for all nodules, and 89% for nodules measuring greater than or equal to 5 mm compared with reference standard PET-CT. Only 38% of nodules less than or equal to 4 mm were detected by PET-MR imaging. In a follow-up study at the same institution, Raad and colleagues<sup>82</sup> reported that 97% of nodules missed on PET-MR imaging resolved or remained stable on follow-up, suggestive of benignity. This suggests that most nodules measuring less than 5 mm are either benign or do not contribute significantly to patient management. Further studies are required to explore this issue and to compare the lower sensitivity of PET-MR imaging for small lung nodules against potentially higher sensitivity in other organs such as the brain, liver, adrenal glands, and bone marrow.

With respect to metastatic lymph node detection with PET-MR imaging, preliminary evidence is emerging. In 2014, Heusch and colleagues<sup>83</sup> studied 22 subjects with lung cancer and reported no statistically significant difference between PET-CT and PET-MR imaging for metastatic lymph node detection. PET-MR imaging correctly staged 20 of 22 subjects versus 18 of 22 for PET-CT. The advantage of PET-MR imaging was not only due to the modality. There was time-dependent FDG washout within an inflammatory node in one subject and, in another subject, a lesion was seen on PET-MR imaging that was not visible on PET-CT. Both modalities missed a small supraclavicular lymph node metastasis.

Detection of distant metastases has been studied extensively in the MR imaging literature. Some studies combine PET findings with separately acquired MR imaging, and various MR imaging techniques, including DWI and contrast-enhanced imaging, have been reported. To date, few studies exist for which patients underwent PET-MR imaging in the same imaging session on a single scanner. Preliminary work with integrated PET-MR imaging scanners or software-fused PET and MR imaging datasets has suggested overall equivalence between PET-MR imaging and PET-CT for distant metastasis detection.<sup>83,84</sup> One group has reported that addition of signal intensity quantification on MR imaging may offer higher performance than routine PET-MR imaging or PET-CT.<sup>85</sup> It is likely that large-scale multi-institutional studies will be required to determine if there is a significant true increase in clinically meaningful distant metastasis detection with PET-MR imaging compared with PET-CT.<sup>85</sup>

## ADDITIONAL PET-MR IMAGING APPLICATIONS IN LUNG CANCER: MULTIPARAMETRIC DATASETS

A potential advantage of PET-MR imaging is that it can deliver quantitatively accurately multiparametric datasets consisting of molecular information from both PET and MR imaging, and that these datasets may improve future patient care. Most of the PET-MR imaging research in this area to date has focused on comparing FDG PET data with that obtained from DWI. The ADC values provided by DWI represent a possible new way to independently or synergistically evaluate tumors during clinical PET-MR imaging.

In 2013, Heusch and colleagues<sup>81</sup> reported a statistically significant inverse correlation between FDG PET SUV and ADC values on PET-MR imaging in subjects with NSCLC. In 2015, Schaarschmidt and colleagues<sup>86</sup> also reported a weak inverse correlation. They suggested the weakness of the correlation suggests that FDG PET and DWI may offer complementary information that may be useful in patients with NSCLC. They discuss that correlations may vary across histologic subtypes and that further research is required to determine how to use this information. Figs. 4–6 give examples of PET-MR imaging in patients with lung cancer.

### SUMMARY

PET-MR imaging is a promising new modality that brings together the advantages of both MR imaging and PET-CT in a single examination, with few limitations. The potential for increased lesion detection, reduced radiation exposure, improved patient convenience, and improved patient management by leveraging of multiparametric quantitative datasets are all compelling reasons to move forward with clinical PET-MR imaging. That being said, PET-CT is already a highly accurate modality, and large studies will likely be required to demonstrate that PET-MR imaging is worth the additional cost and complexity.

For patients with breast cancer, preliminary research suggests that PET-MR imaging can potentially detect additional tumor deposits in at least some patients, particularly in the bone marrow, liver, and brain. A key question is to determine just how often these benefits are realized and in which exact clinical scenarios. It remains to be seen if PET-MR imaging can guide clinicians and patients towards specific therapies or to monitor treatment response in the early stages of therapy. Such applications may require development of new radiotracers that can predict the molecular behavior of breast cancers with higher specificity. Clinical PET-MR imaging in breast cancer is still very much in its infancy.

With respect to lung cancer, it is hard for PET-MR imaging to compete against the near-perfect sensitivity of chest CT for detection of primary lung cancers and metastatic lung nodules. Applications may exist for determining T stage in tumors that abut or invade the mediastinum or chest wall, and in individuals with pre-existing chest CT, there may be value in performing a comprehensive staging study that combines diagnostic MR imaging of the brain, adrenal glands, and liver, with additional bone-marrow specific sequences to comprehensively stage or restage lung cancer. As in the case of breast cancer, it remains to be seen which exact patient populations and at what particular stages of clinical presentation

will benefit from this modality. It is likely that, similar to PET-CT, the benefits of PET-MR imaging will be more likely realized in individuals with moderate-to-high risk for harboring metastatic disease that is invisible by conventional CT or MR imaging. Finally, it remains to be seen if multi-parametric PET-MR imaging can be used to predict or monitor treatment responses in an era in which myriad treatment options exist beyond conventional cytotoxic chemotherapy.

Preliminary research has demonstrated a potential added value of PET-MR imaging compared with PET-CT or MR imaging alone in the staging and restaging of patients with breast cancer and lung cancer but much work remains to be done to determine the specific applications that will allow this modality to flourish and to maximize its potential beyond that of PET-CT.

## References

1. Siegel RL, Miller KD, Jemal A. Cancer statistics, 2015. *CA Cancer J Clin.* 2015; 65(1):5–29. [PubMed: 25559415]
2. Dunphy MPS, Lewis JS. Radiopharmaceuticals in preclinical and clinical development for monitoring of therapy with PET. *J Nucl Med.* 2009; 50:106S–21S. [PubMed: 19380404]
3. Rice SL, Roney CA, Daumar P, et al. The next generation of positron emission tomography radiopharmaceuticals in oncology. *Semin Nucl Med.* 2011; 41(4):265–82. [PubMed: 21624561]
4. Miller WR, Ellis IO, Sainsbury JR, et al. ABC of breast diseases. Prognostic factors. *BMJ.* 1994; 309(6968):1573–6. [PubMed: 7819905]
5. Le-Petross CH, Bidaut L, Yang WT. Evolving role of imaging modalities in inflammatory breast cancer. *Semin Oncol.* 2008; 35(1):51–63. [PubMed: 18308146]
6. Yang WT, Le-Petross HT, Macapinlac H, et al. Inflammatory breast cancer: PET/CT, MRI, mammography, and sonography findings. *Breast Cancer Res Treat.* 2008; 109(3):417–26. [PubMed: 17653852]
7. Avril N, Rosé CA, Schelling M, et al. Breast imaging with positron emission tomography and fluorine-18 fluorodeoxyglucose: use and limitations. *J Clin Oncol.* 2000; 18(20):3495–502. [PubMed: 11032590]
8. Heusner TA, Kuemmel S, Umutlu L, et al. Breast cancer staging in a single session: whole-body PET/CT mammography. *J Nucl Med.* 2008; 49(8):1215–22. [PubMed: 18632831]
9. Scheidhauer K, Walter C, Seemann MD. FDG PET and other imaging modalities in the primary diagnosis of suspicious breast lesions. *Eur J Nucl Med Mol Imaging.* 2004; 31(Suppl 1):S70–9. [PubMed: 15133634]
10. Uematsu T, Kasami M, Yuen S. Comparison of FDG PET and MRI for evaluating the tumor extent of breast cancer and the impact of FDG PET on the systemic staging and prognosis of patients who are candidates for breast-conserving therapy. *Breast Cancer.* 2009; 16(2):97–104. [PubMed: 18663562]
11. Heusner TA, Freudenberg LS, Kuehl H, et al. Whole-body PET/CT-mammography for staging breast cancer: initial results. *Br J Radiol.* 2008; 81(969):743–8. [PubMed: 18508873]
12. Torizuka T, Zasadny KR, Recker B, et al. Untreated primary lung and breast cancers: correlation between F-18 FDG kinetic rate constants and findings of in vitro studies. *Radiology.* 1998; 207(3):767–74. [PubMed: 9609902]
13. Kumar R, Loving VA, Chauhan A, et al. Potential of dual-time-point imaging to improve breast cancer diagnosis with (18)F-FDG PET. *J Nucl Med.* 2005; 46(11):1819–24. [PubMed: 16269595]
14. Mavi A, Urhan M, Yu JQ, et al. Dual time point 18F-FDG PET imaging detects breast cancer with high sensitivity and correlates well with histologic subtypes. *J Nucl Med.* 2006; 47(9):1440–6. [PubMed: 16954551]

15. Wahl RL, Siegel BA, Coleman RE, et al. Prospective multicenter study of axillary nodal staging by positron emission tomography in breast cancer: a report of the staging breast cancer with PET Study Group. *J Clin Oncol.* 2004; 22(2):277–85. [PubMed: 14722036]
16. Schwarz-Dose J, Untch M, Tiling R, et al. Monitoring primary systemic therapy of large and locally advanced breast cancer by using sequential positron emission tomography imaging with [18F]fluorodeoxyglucose. *J Clin Oncol.* 2009; 27(4):535–41. [PubMed: 19075273]
17. Rousseau C, Devillers A, Sagan C, et al. Monitoring of early response to neoadjuvant chemotherapy in stage II and III breast cancer by [18F]fluorodeoxyglucose positron emission tomography. *J Clin Oncol.* 2006; 24(34):5366–72. [PubMed: 17088570]
18. Kamel EM, Wyss MT, Fehr MK, et al. [18F]-Fluorodeoxyglucose positron emission tomography in patients with suspected recurrence of breast cancer. *J Cancer Res Clin Oncol.* 2003; 129(3):147–53. [PubMed: 12712329]
19. Eubank WB, Mankoff D, Bhattacharya M, et al. Impact of FDG PET on defining the extent of disease and on the treatment of patients with recurrent or metastatic breast cancer. *AJR Am J Roentgenol.* 2004; 183(2):479–86. [PubMed: 15269044]
20. Tateishi U, Gamez C, Dawood S, et al. Bone metastases in patients with metastatic breast cancer: morphologic and metabolic monitoring of response to systemic therapy with integrated PET/CT. *Radiology.* 2008; 247(1):189–96. [PubMed: 18372468]
21. Siggelkow W, Zimny M, Faridi A, et al. The value of positron emission tomography in the follow-up for breast cancer. *Anticancer Res.* 2003; 23(2C):1859–67. [PubMed: 12820470]
22. Du Y, Cullum I, Illidge TM, et al. Fusion of metabolic function and morphology: sequential [18F]fluorodeoxyglucose positron-emission tomography/computed tomography studies yield new insights into the natural history of bone metastases in breast cancer. *J Clin Oncol.* 2007; 25(23):3440–7. [PubMed: 17592153]
23. Tillman GF, Orel SG, Schnall MD, et al. Effect of breast magnetic resonance imaging on the clinical management of women with early-stage breast carcinoma. *J Clin Oncol.* 2002; 20(16):3413–23. [PubMed: 12177101]
24. Lehman CD, DeMartini W, Anderson BO, et al. Indications for breast MRI in the patient with newly diagnosed breast cancer. *J Natl Compr Canc Netw.* 2009; 7(2):193–201. [PubMed: 19200417]
25. Weinstein S, Rosen M. Breast MR imaging: current indications and advanced imaging techniques. *Radiol Clin North Am.* 2010; 48(5):1013–42. [PubMed: 20868898]
26. Zeppa R. Vascular response of breast to estrogen. *J Clin Endocrinol Metab.* 1969; 29(5):695–700. [PubMed: 5781782]
27. Vogel PM, Georgiade NG, Fetter BF, et al. The correlation of histologic-changes in the human-breast with the menstrual-cycle. *Am J Pathol.* 1981; 104(1):23–34. [PubMed: 7258295]
28. Giess CS, Yeh ED, Raza S, et al. Background parenchymal enhancement at breast MR imaging: normal patterns, diagnostic challenges, and potential for false-positive and false-negative interpretation. *Radiographics.* 2014; 34(1):234–47. [PubMed: 24428293]
29. Vag T, Baltzer PA, Dietzel M, et al. Kinetic characteristics of ductal carcinoma in situ (DCIS) in dynamic breast MRI using computer-assisted analysis. *Acta Radiol.* 2010; 51(9):955–61. [PubMed: 20942728]
30. Kvistad KA, Rydland J, Vainio J, et al. Breast lesions: evaluation with dynamic contrast-enhanced T1-weighted MR imaging and with T2\*-weighted first-pass perfusion MR imaging. *Radiology.* 2000; 216(2):545–53. [PubMed: 10924584]
31. Kim JA, Son EJ, Youk JH, et al. MRI findings of pure ductal carcinoma in situ: kinetic characteristics compared according to lesion type and histopathologic factors. *AJR Am J Roentgenol.* 2011; 196(6):1450–6. [PubMed: 21606313]
32. Kvistad KA, Rydland J, Smethurst HB, et al. Axillary lymph node metastases in breast cancer: preoperative detection with dynamic contrast-enhanced MRI. *Eur Radiol.* 2000; 10(9):1464–71. [PubMed: 10997438]
33. Pace L, Nicolai E, Luongo A, et al. Comparison of whole-body PET/CT and PET/MRI in breast cancer patients: lesion detection and quantitation of 18F-deoxyglucose uptake in lesions and in normal organ tissues. *Eur J Radiol.* 2014; 83(2):289–96. [PubMed: 24331845]

34. Sawicki LM, Grueneisen J, Schaarschmidt BM, et al. Evaluation of (18)F-FDG PET/MRI, (18)F-FDG PET/CT, MRI, and CT in whole-body staging of recurrent breast cancer. *Eur J Radiol.* 2016; 85(2):459–65. [PubMed: 26781152]
35. Pujara AC, Raad RA, Ponzo F, et al. Standardized uptake values from PET/MRI in metastatic breast cancer: an organ-based comparison with PET/CT. *Breast J.* 2016; 22(3):264–73. [PubMed: 26843433]
36. Melsaether AN, Raad RA, Pujara AC, et al. Comparison of whole-body F FDG PET/MR imaging and whole-body F FDG PET/CT in terms of lesion detection and radiation dose in patients with breast cancer. *Radiology.* 2016 151155. [Epub ahead of print].
37. Minamimoto R, Mosci C, Jamali M, et al. Semiquantitative analysis of the biodistribution of the combined (1)(8)F-NaF and (1)(8)F-FDG administration for PET/CT imaging. *J Nucl Med.* 2015; 56(5):688–94. [PubMed: 25840978]
38. Iagaru A, Minamimoto R, Levin C, et al. The potential of TOF PET-MRI for reducing artifacts in PET images. *EJNMMI Phys.* 2015; 2(Suppl 1):A77. [PubMed: 26956338]
39. Dregely I, Lanz T, Metz S, et al. A 16-channel MR coil for simultaneous PET/MR imaging in breast cancer. *Eur Radiol.* 2015; 25(4):1154–61. [PubMed: 25287263]
40. Moy L, Noz ME, Maguire GQ Jr, et al. Role of fusion of prone FDG-PET and magnetic resonance imaging of the breasts in the evaluation of breast cancer. *Breast J.* 2010; 16(4):369–76. [PubMed: 20443788]
41. Baba S, Isoda T, Maruoka Y, et al. Diagnostic and prognostic value of pretreatment SUV in 18F-FDG/PET in breast cancer: comparison with apparent diffusion coefficient from diffusion-weighted MR imaging. *J Nucl Med.* 2014; 55(5):736–42. [PubMed: 24665089]
42. Miyake KK, Nakamoto Y, Kanao S, et al. Journal club: diagnostic value of (18)F-FDG PET/CT and MRI in predicting the clinicopathologic subtypes of invasive breast cancer. *AJR Am J Roentgenol.* 2014; 203(2):272–9. [PubMed: 25055259]
43. Lim I, Noh WC, Park J, et al. The combination of FDG PET and dynamic contrast-enhanced MRI improves the prediction of disease-free survival in patients with advanced breast cancer after the first cycle of neoadjuvant chemotherapy. *Eur J Nucl Med Mol Imaging.* 2014; 41(10):1852–60. [PubMed: 24927797]
44. Brandman S, Ko JP. Pulmonary nodule detection, characterization, and management with multidetector computed tomography. *J Thorac Imaging.* 2011; 26(2):90–105. [PubMed: 21508732]
45. Zhao F, Yan SX, Wang GF, et al. CT features of focal organizing pneumonia: an analysis of consecutive histopathologically confirmed 45 cases. *Eur J Radiol.* 2014; 83(1):73–8. [PubMed: 23711424]
46. Zhang ZW, Rong EG, Shi MX, et al. Expression and functional analysis of Kruppel-like factor 2 in chicken adipose tissue. *J Anim Sci.* 2014; 92(11):4797–805. [PubMed: 25349335]
47. Eubank WB, Mankoff DA, Schmiedl UP, et al. Imaging of oncologic patients: benefit of combined CT and FDG PET in the diagnosis of malignancy. *Am J Roentgenol.* 1998; 171(4):1103–10. [PubMed: 9763005]
48. De Wever W, Ceyskens S, Mortelmans L, et al. Additional value of PET-CT in the staging of lung cancer: comparison with CT alone, PET alone and visual correlation of PET and CT. *Eur Radiol.* 2007; 17(1):23–32. [PubMed: 16683115]
49. Gould MK, Maclean CC, Kuschner WG, et al. Accuracy of positron emission tomography for diagnosis of pulmonary nodules and mass lesions: a meta-analysis. *JAMA.* 2001; 285(7):914–24. [PubMed: 11180735]
50. Lowe VJ, Fletcher JW, Gobar L, et al. Prospective investigation of positron emission tomography in lung nodules. *J Clin Oncol.* 1998; 16(3):1075–84. [PubMed: 9508193]
51. Patz EF, Lowe VJ, Hoffman JM, et al. Focal pulmonary abnormalities: evaluation with F-18 fluorodeoxyglucose PET scanning. *Radiology.* 1993; 188(2):487–90. [PubMed: 8327702]
52. Erasmus JJ, McAdams HP, Patz EF Jr, et al. Evaluation of primary pulmonary carcinoid tumors using FDG PET. *Am J Roentgenol.* 1998; 170(5):1369–73. [PubMed: 9574618]
53. Higashi K, Ueda Y, Seki H, et al. Fluorine-18-FDG PET imaging is negative in bronchioloalveolar lung carcinoma. *J Nucl Med.* 1998; 39(6):1016–20. [PubMed: 9627336]

54. Kim BT, Kim Y, Lee KS, et al. Localized form of bronchioloalveolar carcinoma: FDG PET findings. *Am J Roentgenol.* 1998; 170(4):935–9. [PubMed: 9530038]
55. Henschke CI, Yankelevitz DF, Kostis WJ. CT screening for lung cancer. *Semin Ultrasound CT MR.* 2003; 24(1):23–32. [PubMed: 12708641]
56. Antoch G, Stattaus J, Nemat AT, et al. Non-small cell lung cancer: dual-modality PET/CT in preoperative staging. *Radiology.* 2003; 229(2):526–33. [PubMed: 14512512]
57. Birim O, Kappetein AP, Stijnen T, et al. Meta-analysis of positron emission tomographic and computed tomographic imaging in detecting mediastinal lymph node metastases in nonsmall cell lung cancer. *Ann Thorac Surg.* 2005; 79(1):375–82. [PubMed: 15620991]
58. Halter G, Buck AK, Schirrmester H, et al. Lymph node staging in lung cancer using [F-18]FDG-PET. *Thorac Cardiovasc Surg.* 2004; 52(2):96–101. [PubMed: 15103582]
59. Lardinois D, Weder W, Hany TF, et al. Staging of non-small-cell lung cancer with integrated positron-emission tomography and computed tomography. *N Engl J Med.* 2003; 348(25):2500–7. [PubMed: 12815135]
60. Bille A, Pelosi E, Skanjeti A, et al. Preoperative intrathoracic lymph node staging in patients with non-small-cell lung cancer: accuracy of integrated positron emission tomography and computed tomography. *Eur J Cardiothorac Surg.* 2009; 36(3):440–5. [PubMed: 19464906]
61. Erasmus JJ, Patz EF Jr, McAdams HP, et al. Evaluation of adrenal masses in patients with bronchogenic carcinoma using F-18-fluorodeoxy-glucose positron emission tomography. *Am J Roentgenol.* 1997; 168(5):1357–60. [PubMed: 9129444]
62. Marom EM, McAdams HP, Erasmus JJ, et al. Staging non-small cell lung cancer with whole-body PET. *Radiology.* 1999; 212(3):803–9. [PubMed: 10478250]
63. Bury T, Corhay JL, Duysinx B, et al. Value of FDG-PET in detecting residual or recurrent nonsmall cell lung cancer. *Eur Respir J.* 1999; 14(6):1376–80. [PubMed: 10624770]
64. Hellwig D, Gröschel A, Graeter TP, et al. Diagnostic performance and prognostic impact of FDG-PET in suspected recurrence of surgically treated non-small cell lung cancer. *Eur J Nucl Med Mol Imaging.* 2006; 33(1):13–21. [PubMed: 16151765]
65. Ryu JS, Choi NC, Fischman AJ, et al. FDG-PET in staging and restaging non-small cell lung cancer after neoadjuvant chemoradiotherapy: correlation with histopathology. *Lung Cancer.* 2002; 35(2):179–87. [PubMed: 11804691]
66. Bergin CJ, Glover GH, Pauly JM. Lung parenchyma: magnetic-susceptibility in MR imaging. *Radiology.* 1991; 180(3):845–8. [PubMed: 1871305]
67. Lauenstein TC, Goehde SC, Herborn CU, et al. Whole-body MR imaging: evaluation of patients for metastases. *Radiology.* 2004; 233(1):139–48. [PubMed: 15317952]
68. Ohno Y, Oshio K, Uematsu H, et al. Single-shot half-Fourier RARE sequence with ultra-short inter-echo spacing for lung imaging. *J Magn Reson Imaging.* 2004; 20(2):336–9. [PubMed: 15269963]
69. Attenberger U, Catana C, Chandarana H, et al. Whole-body FDG PET-MR oncologic imaging: pitfalls in clinical interpretation related to inaccurate MR-based attenuation correction. *Abdom Imaging.* 2015; 40(6):1374–86. [PubMed: 26025348]
70. Kurihara Y, Matsuoka S, Yamashiro T, et al. MRI of pulmonary nodules. *Am J Roentgenol.* 2014; 202(3):W210–6. [PubMed: 24555616]
71. Schroeder T, Ruehm SG, Debatin JF, et al. Detection of pulmonary nodules using a 2D HASTE MR sequence: comparison with MDCT. *Am J Roentgenol.* 2005; 185(4):979–84. [PubMed: 16177419]
72. Koyama H, Ohno Y, Kono A, et al. Quantitative and qualitative assessment of non-contrast-enhanced pulmonary MR imaging for management of pulmonary nodules in 161 subjects. *Eur Radiol.* 2008; 18(10):2120–31. [PubMed: 18458913]
73. Fujimoto K, Abe T, Müller NL, et al. Small peripheral pulmonary carcinomas evaluated with dynamic MR imaging: correlation with tumor vascularity and prognosis. *Radiology.* 2003; 227(3):786–93. [PubMed: 12714678]
74. Kono R, Fujimoto K, Terasaki H, et al. Dynamic MRI of solitary pulmonary nodules: comparison of enhancement patterns of malignant and benign small peripheral lung lesions. *Am J Roentgenol.* 2007; 188(1):26–36. [PubMed: 17179342]

75. Uto T, Takehara Y, Nakamura Y, et al. Higher sensitivity and specificity for diffusion-weighted imaging of malignant lung lesions without apparent diffusion coefficient quantification. *Radiology*. 2009; 252(1):247–54. [PubMed: 19420317]
76. Koyama H, Ohno Y, Aoyama N, et al. Comparison of STIR turbo SE imaging and diffusion-weighted imaging of the lung: capability for detection and subtype classification of pulmonary adenocarcinomas. *Eur Radiol*. 2010; 20(4):790–800. [PubMed: 19763578]
77. Mori T, Nomori H, Ikeda K, et al. Diffusion-weighted magnetic resonance imaging for diagnosing malignant pulmonary nodules/masses: comparison with positron emission tomography. *J Thorac Oncol*. 2008; 3(4):358–64. [PubMed: 18379353]
78. Schrevels L, Lorent N, Dooms C, et al. The role of PET scan in diagnosis, staging, and management of non-small cell lung cancer. *Oncologist*. 2004; 9(6):633–43. [PubMed: 15561807]
79. Chandarana H, Heacock L, Rakheja R, et al. Pulmonary nodules in patients with primary malignancy: comparison of hybrid PET/MR and PET/CT imaging. *Radiology*. 2013; 268(3):874–81. [PubMed: 23737537]
80. Kohan AA, Kolthammer JA, Vercher-Conejero JL, et al. N staging of lung cancer patients with PET/MRI using a three-segment model attenuation correction algorithm: initial experience. *Eur Radiol*. 2013; 23(11):3161–9. [PubMed: 23765261]
81. Heusch P, Köhler J, Wittsack HJ, et al. Hybrid [(1)(8)F]-FDG PET/MRI including non-Gaussian diffusion-weighted imaging (DWI): preliminary results in non-small cell lung cancer (NSCLC). *Eur J Radiol*. 2013; 82(11):2055–60. [PubMed: 23830904]
82. Raad RA, Friedman KP, Heacock L, et al. Outcome of small lung nodules missed on hybrid PET/MRI in patients with primary malignancy. *J Magn Reson Imaging*. 2016; 43(2):504–11. [PubMed: 26192731]
83. Heusch P, Buchbender C, Köhler J, et al. Thoracic staging in lung cancer: prospective comparison of 18F-FDG PET/MR imaging and 18F-FDG PET/CT. *J Nucl Med*. 2014; 55(3):373–8. [PubMed: 24504054]
84. Lee SM, Goo JM, Park CM, et al. Preoperative staging of non-small cell lung cancer: prospective comparison of PET/MR and PET/CT. *Eur Radiol*. 2016 [Epub ahead of print].
85. Ohno Y, Koyama H, Yoshikawa T, et al. Three-way comparison of whole-body MR, coregistered whole-body FDG PET/MR, and integrated whole-body FDG PET/CT Imaging: TNM and stage assessment capability for non-small cell lung cancer patients. *Radiology*. 2015; 275(3):849–61. [PubMed: 25584709]
86. Schaarschmidt BM, Buchbender C, Nensa F, et al. Correlation of the apparent diffusion coefficient (ADC) with the standardized uptake value (SUV) in lymph node metastases of non-small cell lung cancer (NSCLC) patients using hybrid 18F-FDG PET/MRI. *PLoS One*. 2015; 10(1):e0116277. [PubMed: 25574968]



**KEY POINTS**

- PET-MR imaging may potentially detect more distant metastases in breast cancer compared with PET-CT or MR imaging alone, and it has the potential to guide breast biopsies based on higher specificity compared with MR imaging.
- PET-MR imaging has the potential to detect distant metastases of lung cancer with even higher sensitivity than PET-CT or MR imaging alone.
- Current PET-MR imaging systems will not replace chest computed tomography (CT) for detection of small primary lung tumors.
- PET-MR imaging offers advantages compared with PET-CT with respect to molecular-anatomic lesion registration, motion correction, radiation dose, and patient convenience.
- PET-MR imaging has the potential to allow precise quantification of molecular information obtained by both PET and MR imaging, and allows for voxelwise correlation and temporally aligned data that may inform patient management in the future.

**Box 1****Typical breast cancer or lung cancer PET-MR imaging protocol**

- 15 mCi  $^{18}\text{F}$ - 2-fluoro-2-deoxy-D-glucose (FDG) intravenously, wait 60 minutes, void
  - Can perform diagnostic breast MR imaging during radiotracer uptake period if desired (for patients with breast cancer)
- Scan from skull vertex to thighs
- Multichannel head and neck coil, flexible body coil
- 6 minutes per bed PET acquisition with simultaneous MR imaging sequences
  - Dixon MR imaging attenuation correction images
  - 3-dimensional T1-weighted images
  - 3 b-value diffusion-weighted imaging (DWI)
  - Axial T2-weighted half-Fourier single-shot turbo spin echo (HASTE) or short tau inversion recovery (STIR) images if desired by imaging physician
- Inject gadolinium-based contrast material intravenously
  - Postcontrast 3-dimensional T1-weighted images of liver and brain

**Box 2****PET-MR imaging pitfalls in breast and lung cancers**

- Metallic artifacts in breast tissue expanders can generate signal dropout on attenuation maps and result in underestimation of standardized uptake value (SUV) in chest wall lesions.
- Misclassification of lung tissue as air can underestimate SUV in lung lesions.
- Misclassification of hilar lymph nodes as air can result in SUV underestimation.
- Clinical PET-MR imaging readers should keep in mind the breath-hold protocol for various sequences obtained during PET-MR imaging and understand the potential for lesion misregistration relative to PET.
- MR imaging motion-tracking holds great promise for motion correction of PET datasets in the near future, without additional radiation exposure.
- Geometric distortion on DWI datasets results in misregistration to PET data; this should be kept in mind during clinical interpretation.

**Box 3**

**What the referring physician needs to know about PET-MR imaging**

- PET-MR imaging performance is comparable to PET-CT in breast cancer and lung cancer.
- Preliminary evidence suggests a potential advantage of PET-MR imaging in detection of brain, bone marrow, liver, and adrenal gland metastases in breast cancer and lung cancer.
- Increased sensitivity in these organs comes at a cost of lower sensitivity for small lung metastases.
- PET-MR imaging examinations offer a convenient study for patients who require both PET and MR imaging, with reduced radiation exposure and potentially shorter total scan time compared with separate PET-CT and MR imaging.
- PET-MR imaging allows generation of multi-parametric quantitative datasets; preliminary research suggests possible synergy between SUV, DWI, and contrast-enhanced MR imaging parameters; however, future research is required before quantitative PET-MR imaging will directly influence patient management.

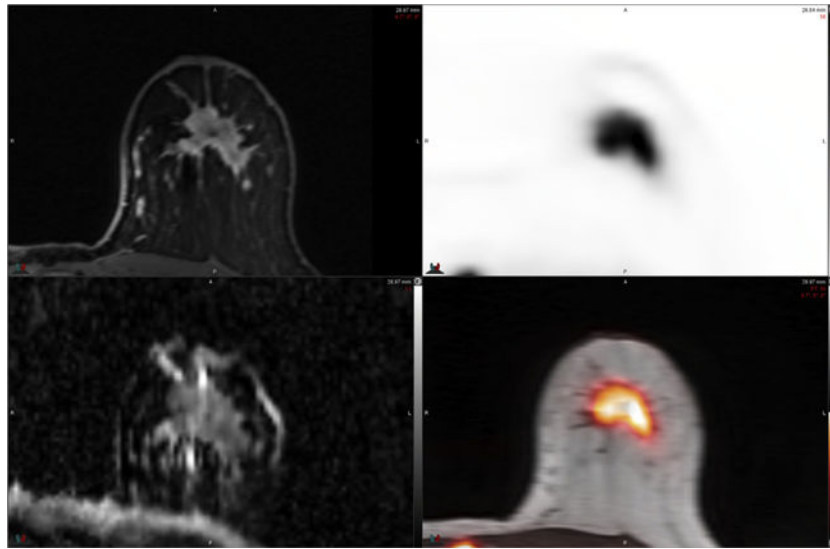


**Fig. 1.** 54-year-old woman with newly diagnosed left breast cancer. FDG PET-MR imaging performed in the prone position (reoriented) with a dedicated breast coil demonstrates intense FDG uptake in primary tumor on PET and PET-MR images (*top right* and *bottom right*). ADC map MR image (*bottom left*) demonstrates heterogeneous signal intensity with areas of low ADC (*grey-black regions*) within tumor due to high cellularity. Postcontrast T1-weighted MR image (*top left*) demonstrates heterogeneous enhancement within the mass. Prone PET-MR imaging with dedicated breast coil facilitates multiparametric quantitative analysis of primary breast tumors. (*Courtesy of Dr Amy Melsaether, NYU Langone Medical Center, New York, NY.*)

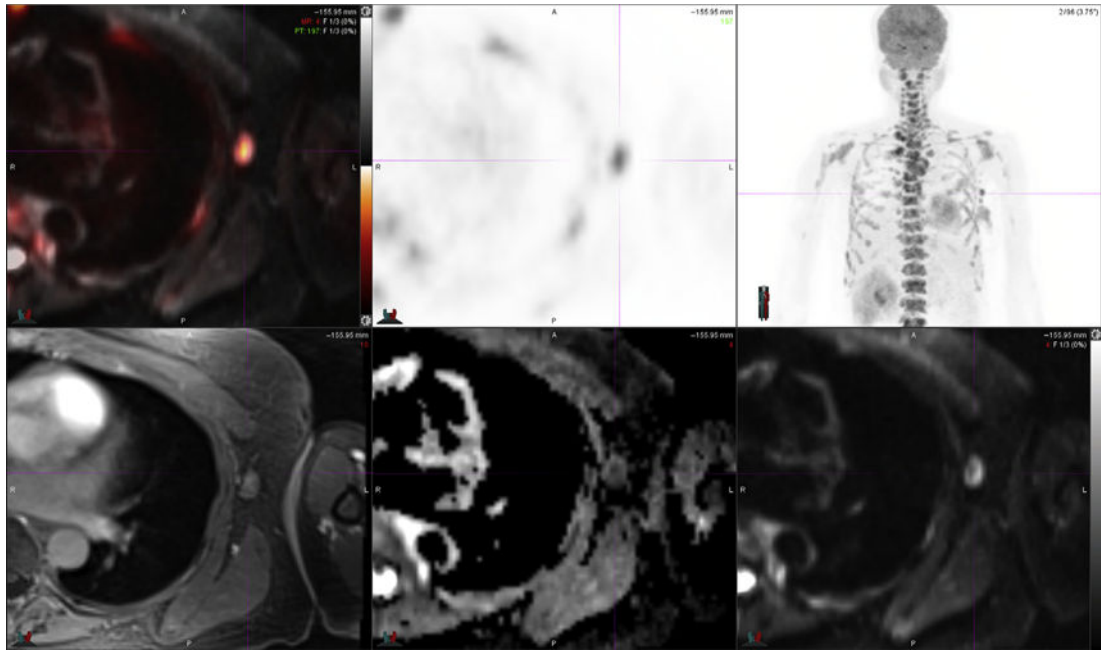


**Fig. 2.** Left axillary lymph node metastasis in patient presented in Fig. 1. FDG PET-MR image (*top left*) and PET images (*top middle* and *top right*) demonstrate intense radiotracer uptake in a borderline prominent left axillary node. T1-weighted fat-suppressed MR image (*bottom left*) demonstrates isointense signal intensity of lymph node relative to skeletal muscle. DWI MR image (*bottom right*) demonstrates high signal intensity of lymph node, and resulting ADC map MR image (*bottom middle*) demonstrates low signal intensity within central portion of the lymph node in keeping with restricted diffusion. (*Courtesy of Dr Amy Melsaether, NYU Langone Medical Center, New York, NY.*)

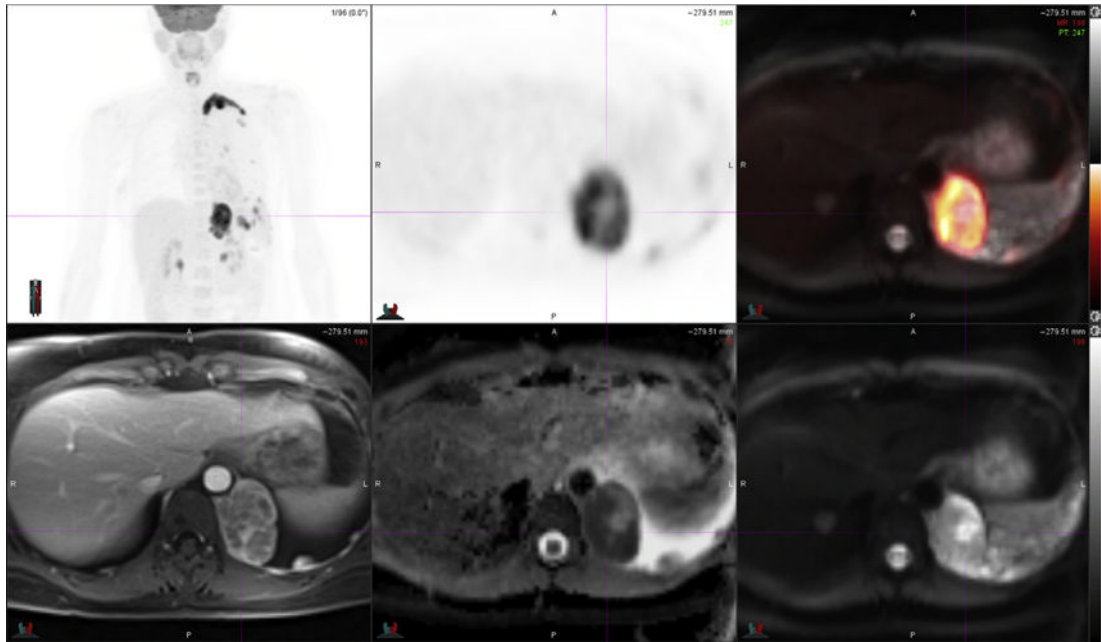


**Fig. 3.** 51-year-old woman with metastatic left breast cancer. FDG PET images (*top left* and *top middle*) and PET-MR image (*top right*) demonstrate large left lung and left pleural metastases, which demonstrate enhancement on post-contrast T1-weighted fat suppressed MR image (*bottom left*). Note that peripheral rim of FDG uptake in lung metastasis corresponds to regions of high cellularity with restricted diffusion on ADC map MR image (*bottom middle*) derived from DWI MR images (*bottom right*). (Courtesy of Dr Amy Melsaether, NYU Langone Medical Center, New York, NY.)

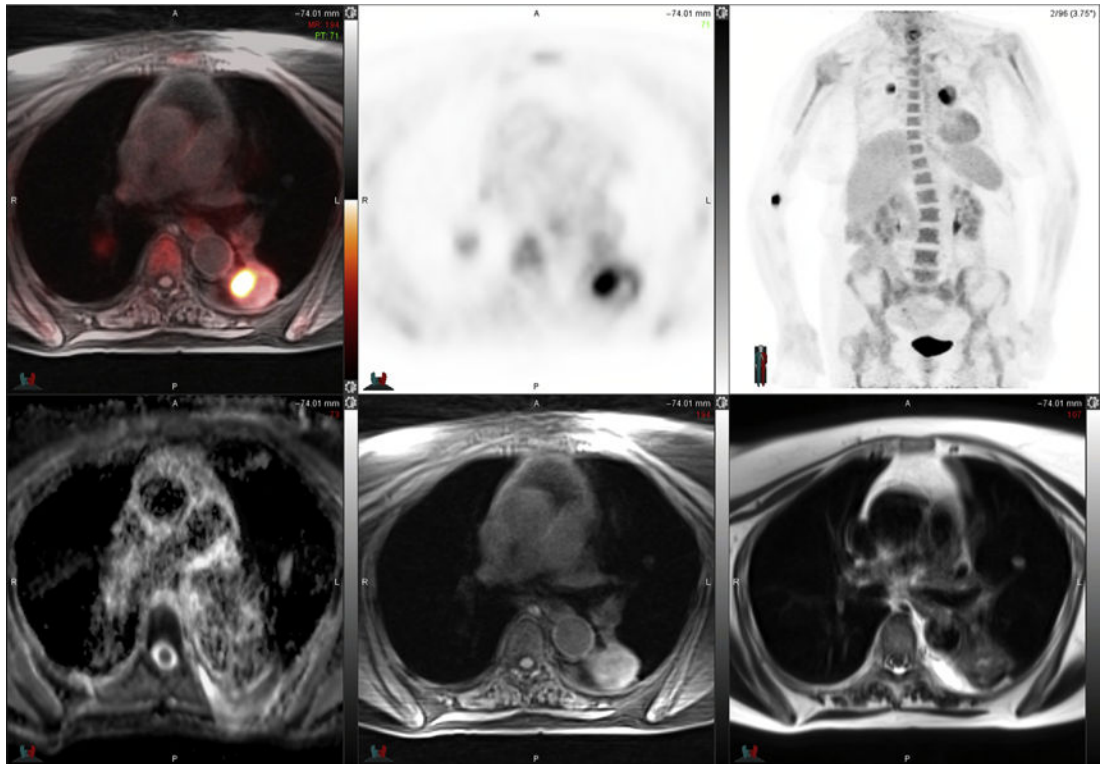


**Fig. 4.** 78-year-old woman with bilateral lung cancers. FDG PET-MR image (*top left*) and PET images (*top middle* and *top right*) demonstrate peripheral intense radiotracer uptake in left lung tumor that is most intense medially. ADC map MR image (*bottom left*) is degraded by motion artifact, a significant challenge for lung nodule imaging. T1-weighted fat-suppressed MR image (*bottom middle*) and T2-weighted MR image (*bottom right*) demonstrate heterogeneous signal intensity in the left lower lobe mass.



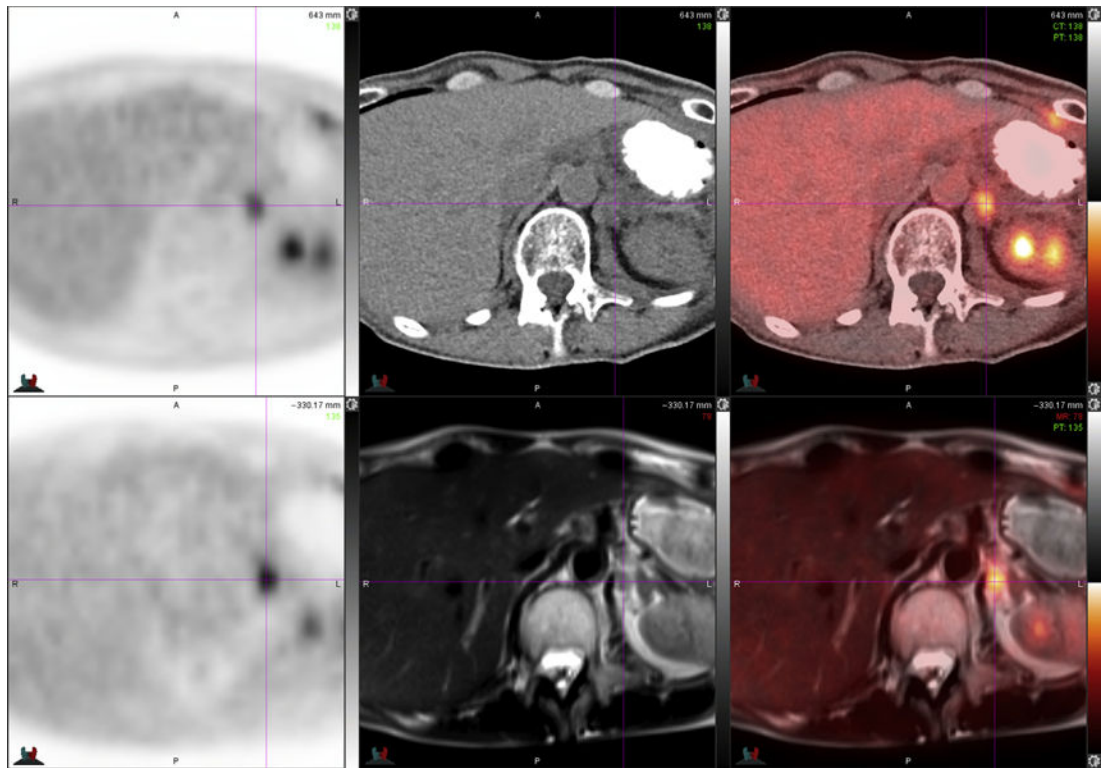


**Fig. 5.** 64-year-old woman with NSCLC. FDG PET-CT images (*top row*) demonstrate presumed left adrenal gland metastasis, which is not well-delineated on low-dose unenhanced CT image (*top middle*) due to relatively low contrast relative to surrounding diaphragm. FDG PET-MR images (*bottom row*) clearly demonstrate that lesion is a retroperitoneal lymph node (*crosshairs*) just medial to the left adrenal gland (darker inverted V-shaped structure lateral to crosshairs). Improved soft tissue contrast of MR imaging yielded better lesion localization compared with PET-CT.

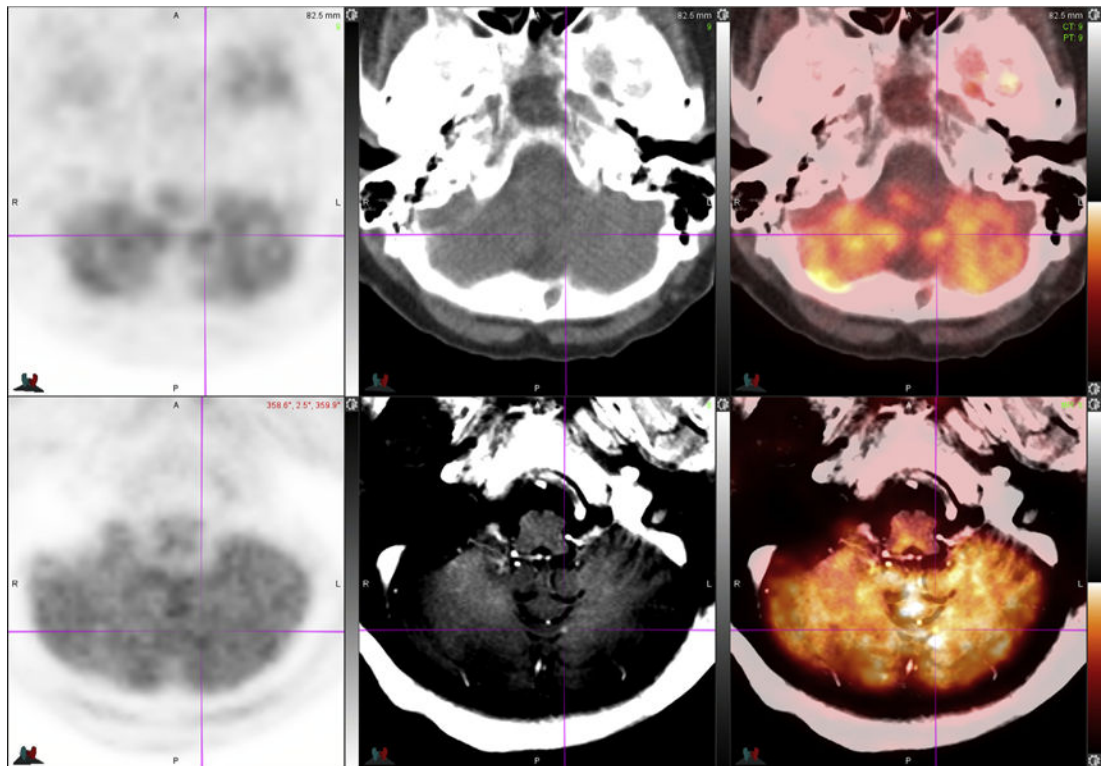


**Fig. 6.** 70-year-old woman with NSCLC. FDG PET-MR images (*bottom row*) identify an enhancing tiny new left cerebellar brain metastasis seen only on postcontrast T1-weighted MR image (*bottom middle*, see crosshair) and PET-MR image (*bottom right*, see crosshair). Note that the lesion is not visible on PET images (*left column*), low-dose unenhanced CT image (*top middle*), or on PET-CT image (*top right*).